

Articles

Dynamics of Methyl Groups in Proteins As Studied by Proton-Detected ^{13}C NMR Spectroscopy. Application to the Leucine Residues of Staphylococcal Nuclease[†]Linda K. Nicholson,[†] Lewis E. Kay,^{*,§,||} Donna M. Baldisseri,[†] Julian Arango,[‡] Paul E. Young,[‡] Ad Bax,[§] and Dennis A. Torchia^{*,†}*Bone Research Branch, National Institute of Dental Research, and Laboratory of Chemical Physics, National Institute of Diabetes and Digestive and Kidney Diseases, National Institutes of Health, Bethesda, Maryland 20892, and the Department of Chemistry, York College, City University of New York, Jamaica, New York 11451**Received February 4, 1992; Revised Manuscript Received March 13, 1992*

ABSTRACT: This paper describes the application of recently developed nuclear magnetic resonance (NMR) pulse sequences to obtain information about the internal dynamics of isotopically enriched hydrophobic side chains in proteins. The two-dimensional spectra provided by the pulse sequences enable one to make accurate measurements of nuclear Overhauser effects (NOE) and longitudinal (T_1) and transverse (T_2) relaxation times of enriched methyl carbons in proteins. Herein, these techniques are used to investigate the internal dynamics of the 11 leucine side chains of staphylococcal nuclease (SNase), a small enzyme having $M_r = 16.8\text{K}$, in the absence and presence of ligands thymidine 3',5'-bisphosphate (pdTp) and Ca^{2+} . We report the synthesis of $[5,5\text{-}^{13}\text{C}_2]\text{leucine}$, the preparation of SNase containing the labeled leucine, the sequential assignment of the leucine methyl carbons and protons in the liganded and unliganded proteins, and the measurement of the ^{13}C T_1 , T_2 , and NOE values for the SNase leucine methyl carbons. Analysis of the relaxation parameters using the formalism of Lipari and Szabo shows that the internal motions of the leucine methyl carbons are characterized by effective correlation times τ_f (5–80 ps) and τ_s (<2 ns). The fast motion is identified with the rapid rotation of the methyl group about the $\text{C}^\gamma\text{-C}^\delta$ bond axis, while the slow motion is associated with reorientation of the $\text{C}^\gamma\text{-C}^\delta$ bond axis itself. The mean squared order parameters associated with the latter motion, S_s^2 , lie in the range 0.34–0.92. The values of S_s^2 correlate reasonably well with the temperature factors of the leucine methyl carbons obtained from the crystal structures, but some are smaller than anticipated on the basis of the fact that nearly all leucine methyl carbons are buried and have temperature factors no larger than that of the leucine backbone atoms. Five leucine residues in liganded SNase and eight in unliganded SNase have values of S_s^2 less than 0.71. These order parameters correspond to large amplitude motions (angular excursions of 27–67°) of the $\text{C}^\gamma\text{-C}^\delta$ bond axis. These results indicate that, in solution, the internal motions of the leucine side chains of SNase are significantly larger than suggested by the X-ray structures or by qualitative analysis of NOESY spectra. Comparison of S_s^2 values obtained from liganded and unliganded SNase reveals a strong correlation between ΔS_s^2 and distance between the leucine methyl carbon and the ligands. A significant increase in S_s^2 upon ligand binding occurs exclusively in those leucine side chains in the vicinity (<10 Å) of either the Ca^{2+} atom or the pdTp heavy atoms, indicating a localized stiffening of the protein structure in regions near the ligand-binding sites.

Recent advances in multidimensional NMR spectroscopy together with isotopic enrichment techniques have enabled one to obtain essentially complete assignments of protons and heteronuclei (^{15}N and ^{13}C) in proteins having a molecular mass in the 15–20 kDa range (Ikura et al., 1990; Kay et al., 1990a; Clore et al., 1990a). The proton assignments together with NOE distance constraints have permitted the first detailed studies of the solution structures of such proteins. The backbone dynamics of SNase (Kay et al., 1989) and interleukin 1 β (Clore et al., 1990b,c) have been investigated using

measurements of ^{15}N T_1 , T_2 , and NOE values of assigned backbone amides, while backbone dynamics of a zinc finger DNA-binding domain from Xfin (Palmer et al., 1991a) have been investigated through the measurement of $^{13}\text{C}_\alpha$ T_1 , T_2 , and NOE values. The recent availability of ^{13}C assignments of amino acid side chains using HCCH-COSY (Kay et al., 1990b) and HCCH-TOCSY spectroscopy (Bax et al., 1990a) now permits similar studies of the dynamics of protein side chains.

Pioneering studies of the internal dynamics of methyl carbons in myoglobin (Jones et al., 1976) and BPTI (Richarz et al., 1980) suggested that a number of large hydrophobic side chains in these proteins had significant internal motions in addition to rotation of the methyl group. SNase contains 11 leucine residues which are, according to the crystal structures of liganded (Loll & Lattman, 1989) and unliganded (Hynes & Fox, 1991) SNase, nearly all buried within the closely packed interior of the protein. The surfaces of a few methyl groups are partially accessible to solvent, and the temperature factors of the leucine methyl carbons do vary significantly from one leucine residue to another. However, in all cases the

[†] This work was supported by the Intramural AIDS Antiviral Program of the Office of the Director of the National Institutes of Health (A.B. and D.A.T.) and by PHS Grant RR08153 (J.A. and P.E.Y.). L.E.K. acknowledges financial support from the Medical Research Council of Canada.

* To whom correspondence should be addressed.

[†] Bone Research Branch, National Institute of Dental Research.

[§] Laboratory of Chemical Physics, NIDDK.

^{||} Present address: Departments of Medical Genetics, Biochemistry and Chemistry, Medical Sciences Building, University of Toronto, Toronto, Ontario, Canada M5S 1A8.

[‡] City University of New York.

leucine methyl carbon temperature factors are no larger than the temperature factors of the leucine backbone atoms. We therefore sought to determine the order parameters of the leucine methyl carbons in solution in order to compare them with the temperature factors. A related goal was to use the order parameters to obtain estimates of the amplitudes of the internal motions of the leucine side chains to determine if they are highly constrained in solution, as suggested by the X-ray data, or flexible like a number of the larger hydrophobic side chains of myoglobin and BPTI in solution.

In order to study the dynamics of the SNase leucine methyl carbons, [5,5'-¹³C₂]leucine was synthesized and biosynthetically incorporated into SNase. Sequential assignments of SNase liganded to pdTp and Ca²⁺ were obtained from a variety of 2D and 3D NMR experiments of the protein labeled at the leucine methyl carbons or uniformly enriched (99%) with ¹³C. The assignments were extended to the unliganded protein using information from the crystal structures and ¹³C-edited NOESY spectra of the proteins containing the labeled leucines. The edited NOESY spectra and the interproton distances obtained from the crystal structures also provided stereospecific assignments of the methyl carbons. Pulse sequences specifically designed to measure relaxation parameters of heteroatoms in AX₃ spin systems with proton detection were used to obtain the *T*₁, *T*₂, and NOE values of the leucine methyl carbons (Palmer et al., 1991b; Kay et al., 1992). The NMR relaxation data were analyzed using the formalism of Lipari and Szabo (Lipari & Szabo, 1982a,b; Clore et al., 1990b) in order to obtain order parameters for the internal motions of the leucine methyl carbons. The internal motion of each leucine methyl carbon was characterized by an order parameter *S* = *S*_γ*S*_β, where *S*_γ is the order parameter for methyl rotation and *S*_β is the order parameter for motion of the C^γ-C^β bond axis. Three physically plausible models of leucine side chain motion were used to obtain estimates of the minimum angular amplitudes of the motions of the C^γ-C^β bond axes. The order parameters obtained for the leucine side chains in liganded and unliganded SNase are compared in order to evaluate the effect of ligation on dynamics of hydrophobic regions scattered throughout the protein. The order parameters are also compared with the SNase temperature factors, and the motional amplitudes derived from the order parameters are compared with previous estimates of amplitudes of internal motions of large hydrophobic side chains in myoglobin and BPTI.

MATERIALS AND METHODS

Synthesis of D,L-[5,5'-¹³C₂]Leucine. The ¹³C-labeled leucine was synthesized by condensation of ethyl acetamidocyanacetate and labeled isobutyl bromide and subsequent hydrolysis. The halide was made from diethyl malonate and ¹³C-labeled methyl iodide (MSD Isotopes) as described in detail in the Supplementary Material. All products were characterized by proton magnetic resonance at 60 and 200 MHz and carbon magnetic resonance at 50 MHz. The overall yield of the product was 1.6%.

Preparation of Labeled SNase. A sample of SNase containing five types of amino acids selectively labeled with ¹⁵N or ¹³C was prepared by growing transformed N4830 *Escherichia coli* in M9 medium, as described previously (Torchia et al., 1989a). The medium was supplemented with all 20 naturally occurring (unlabeled) amino acids (200 mg/L, Sigma Chemical Co.) except Ser, Lys, Gly, Tyr, and Leu. The selectively labeled amino acids, added ca. 15 min prior to thermal induction of protein synthesis, were as follows: L-[¹⁵N]Lys (67 mg/L), [¹⁵N]Gly (133 mg/L); L-[¹³C]Tyr (40

mg/L), and D,L-[5,5'-¹³C₂]Leu (40 mg/L). Except for the Leu, the labeled amino acids were obtained from MSD Isotopes. SNase was purified by ion exchange (S-Sepharose, Pharmacia) and affinity chromatography (Torchia et al., 1989a). A 1.5-L growth yielded 23 mg of purified SNase. Two solutions were prepared for NMR spectroscopy, each with the following composition: SNase, 1.6 mM; NaCl, 100 mM; borate buffer, 50 mM in 99.996% ²H₂O, pD 7.0. One solution also contained the ligands 3',5'-thymidine bisphosphate (pdTp), 5 mM, and Ca²⁺, 10 mM.

NMR Spectroscopy. All spectra were recorded at 500 MHz on a modified Bruker AM500 spectrometer operating in the reverse mode. Quadrature in *F*₁ was achieved via TPPI (Marion & Wüthrich, 1983). Typical 90° pulse widths were 18 μs, ¹H; 35 μs, high-power ¹³C; 170 μs, low-power ¹³C for decoupling.

A number of 2D and 3D NMR experiments were employed to obtain sequential assignments of the leucine methyl groups in SNase. Published pulse sequences were used to record [¹H-¹³C]HMQC (Bax et al., 1990b) and HMQC-RELAY (Lerner & Bax, 1986) spectra. The RELAY was achieved with a WALTZ-17 mixing sequence; mixing times were 29 and 44 ms. ¹³C-edited NOESY (Bax & Weiss, 1987) and ¹³C-edited HMQC-NOESY spectra were obtained using mixing times of 67, 100, and 150 ms. The ¹³C edited HMQC-NOESY pulse scheme consists of a [¹H-¹³C]HMQC pulse sequence (which yields ¹³C chemical shift evolution in *t*₁) followed by an NOE mixing period and proton detection in *t*₂. During *t*₂, WALTZ-16 modulation (Shaka et al., 1983) was used to decouple ¹³C from protons. The NMR data were processed using the Bruker DISNMR software package. Lorentzian to Gaussian digital filtering was used in *t*₁ and in *t*₂.

Newly developed pulse sequences (Figure 1) were used to record ¹³C *T*₁, *T*₂, and NOE values for the leucine methyl carbons in SNase. The experiments are modified versions of pulse sequences originally proposed for the measurement of relaxation times and NOEs of heteroatoms (Kay et al., 1989). Magnetization originating on the low γ heteronucleus is transferred to the directly bound protons for detection via an INEPT transfer sequence (Palmer et al., 1991b; Kay et al., 1992a,b), thereby increasing the sensitivity of the measurements by a factor of (γ_H/γ_C)^{1.5} over direct detection of the heteroatom. In addition, the sensitivity of the experiment is improved by saturation of the proton spins at the start of the sequence to allow for the development of the full ¹H-¹³C NOE. For the leucine methyl carbons studied, this results in a signal enhancement of approximately 2.5-fold. Furthermore, saturation of the protons prior to the start of the experiment effectively suppresses magnetization originating from protons that are not directly coupled to ¹³C spins.

For the pulse schemes shown, special care must be taken to ensure that all existing ¹³C transitions make equal contributions to the observed magnetization and to minimize the effects of cross-correlation and multiexponential proton relaxation on the measured relaxation times (Kay et al., 1992a). The delay τ is chosen to satisfy the equation 2π*J*_{CH}τ = 0.955 rad (54.7°), where *J*_{CH} is the one-bond ¹H-¹³C coupling constant, so that magnetization from each ¹³C single-quantum transition will be transferred equally to ¹H magnetization for observation (Palmer et al., 1991b; Kay et al., 1992a). This is necessary in order to obtain relaxation rates from polarization transfer sequences that are identical to rates measured via ¹³C direct-observe experiments (Kay et al., 1992a). The extraction of accurate ¹³C relaxation rates of methyl groups is further complicated by the effects of (a) cross-correlation

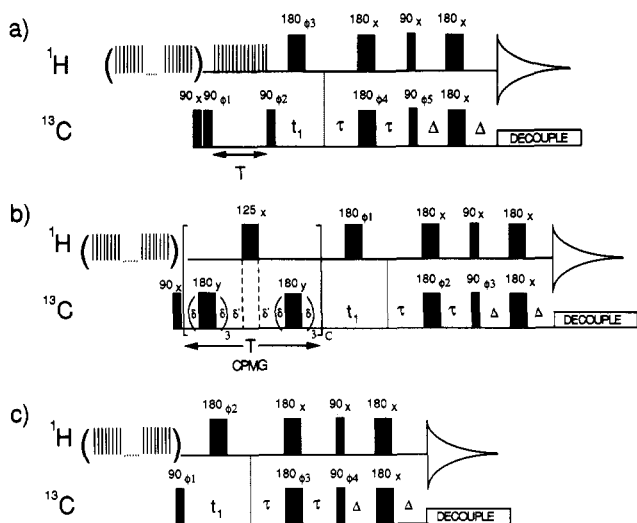


FIGURE 1: Schemes for the measurement of methyl ^{13}C T_1 (a), T_2 (b), and NOE (c) values with ^1H detection. The value of τ is chosen to satisfy the equation $2\pi J_{\text{CH}}\tau = 54.7^\circ$ ($\tau = 1.171$ ms, in this application), and Δ is set to $1/(8J_{\text{CH}})$ to minimize the effects of differential ^1H relaxation (Kay et al., 1992a). ^1H saturation is employed to enhance sensitivity via the NOE and to help suppress magnetization originating from protons not directly coupled to ^{13}C . This is achieved by the application of 125° ^1H pulses spaced at 5-ms intervals for 1.5 s prior to the application of the first ^{13}C pulse (Markley et al., 1971). Cross-correlation effects are minimized by the application of ^1H 125° pulses every 5 ms during the inversion-recovery period. The phase cycling employed for sequence a is $\phi_1 = x,-x$; $\phi_2 = x$; $\phi_3 = 8(x),8(-x)$; $\phi_4 = 2(x),2(y),2(-x),2(-y)$; $\phi_5 = 8(y),8(-y)$; $\text{acq} = 2(x,-x,-x,-x),2(-x,x,x,-x)$. A composite 180° ($90_x 180_y 90_x$) pulse is applied in the middle of the t_1 evolution period. The effect of phase alternation of ϕ_1 is to alternately store magnetization along the $+Z$ axis and the $-Z$ axis so that magnetization relaxes as $\exp(-T/T_1)$. In this way, a nonoptimal delay between scans will only affect the sensitivity of the experiment without introducing systematic errors (Sklenar et al., 1987). Quadrature is achieved by a TPPI of ϕ_2 . The phase cycle for sequence b is $\phi_1 = 4(x),4(-x)$; $\phi_2 = x,y,-x,-y$; $\phi_3 = 8(y),8(-y)$; $\text{acq} = 2(x,-x,x,-x),2(-x,x,-x,x)$. The 180° pulse applied in the center of the t_1 period is of the composite type. Quadrature is achieved by a TPPI of ϕ_3 . The effects of cross-correlation between ^1H - ^{13}C dipolar and CSA interactions and between different ^1H - ^{13}C dipolar interactions are minimized by the application of a ^1H 125° pulse at the height of the spin echo during the CPMG interval every 3.5 ms (Kay et al., 1992a). Within the CPMG sequence, a delay between ^{13}C 180° pulses of 400 μs is employed to ensure that the ^{13}C magnetization remains in phase for the duration of the CPMG interval (Kay et al., 1992a). In order to measure ^1H - ^{13}C NOEs, data sets with and without ^1H saturation are recorded. Scheme c indicates the sequence used for the case of ^1H saturation. In this case, a relaxation delay of 3 s is used, followed by proton presaturation for 3.5 s prior to the first ^{13}C pulse. For the spectra where no NOE is recorded, a delay of 6.5 s is employed between scans. The phase cycle is $\phi_1 = x$; $\phi_2 = 4(x),4(-x)$; $\phi_3 = x,y,-x,-y$; $\phi_4 = 8(y),8(-y)$; $\text{acq} = 2(x,-x,x,-x),2(-x,x,-x,x)$. A composite pulse is employed in the middle of the t_1 evolution, and quadrature is achieved by TPPI of ϕ_1 .

between ^1H - ^{13}C dipolar interactions and (b) cross-correlation between ^1H - ^{13}C dipolar interactions and ^{13}C chemical shift anisotropy (CSA). These effects are minimized by the application of ^1H 125° pulses every ~ 5 ms during the longitudinal recovery period in the sequence of Figure 1a and by the application of ^1H 125° pulses every ~ 5 ms at the height of the spin echo during the CPMG (Carr-Purcell-Meiboom-Gill) period in the sequence of Figure 1b (Carr & Purcell, 1954; Kay et al., 1992a,b). In addition, the delay Δ is set to $1/(8J_{\text{CH}})$ in order to minimize the effects due to differential ^1H relaxation of proton transitions in the methyl group, rather than a value of $1/(4J_{\text{CH}})$, which is optimal for sensitivity. For application to the measurement of ^{13}C relaxation rates of methyl groups in macromolecules, it is often the case that the fastest decaying components of ^1H magnetization are on the

order of the delays used in the polarization transfer experiments. As has been discussed elsewhere (Kay et al., 1992a), this can result in substantial errors in measured relaxation rates. For this reason pulse schemes based on double polarization transfer ($^1\text{H} \rightarrow ^{13}\text{C} \rightarrow ^1\text{H}$) (Kay et al., 1989; Nirmala & Wagner, 1988, 1989) or schemes relying on DEPT transfer cannot be employed. In contrast, the reverse-INEPT polarization transfer experiments of Figure 1 give accurate results (Kay et al., 1992a).

In order to obtain T_1 relaxation rates, seven spectra were acquired with T delays of 10, 50, 110, 170, 260, 350, and 490 ms. T_2 values were obtained from 10 spectra acquired with T delays of 3.8, 11.2, 18.8, 26.3, 33.8, 41.4, 48.9, 79.0, 101.5, and 127.8 ms. All data sets were recorded as 256×512 real matrices with 16 scans per t_1 point. The T_1 , T_2 , and NOE data sets were processed with software provided by New Methods Research (Syracuse, NY). Volumes of cross-peaks were obtained from peak-picking and surface-fitting routines provided in the software package. T_1 values were extracted in a straightforward fashion by measuring the volumes of cross-peaks in 2D maps as a function of the relaxation delay, T , and fitting the volumes to an equation of the form $y = A \exp(-T/T_1)$ using conjugate gradient minimization techniques (Press et al., 1988). The transverse ^{13}C relaxation of an isolated methyl group rapidly rotating about the methyl 3-fold axis and attached to a macromolecule is biexponential, with a fast and a slow time constant corresponding to the inner and outer ^{13}C transitions (Kay et al., 1992a). Therefore, T_2 values were determined by fitting the peak volumes to a biexponential equation of the form $y = 0.5A[\exp(-T/T_{2f}) + \exp(-T/T_{2s})]$, yielding an average initial transverse relaxation rate of $T_{2\text{avg}} = [0.5(T_{2s}^{-1} + T_{2f}^{-1})]^{-1}$. T_2 values were also determined by fitting the peak volumes for the first five time points to a single-exponential equation, yielding the approximate initial relaxation rate. The minimum T_2 value obtained from the single-exponential and biexponential fits for each site ($T_{2\text{min}}$) was used in the analysis of order parameters and correlation times, resulting in the minimum degree of motion for a given site. Precision limits of the extracted parameters, A and T_i ($i = 1, 2_{\text{min}}$), were obtained by a Monte Carlo approach described by Kamath and Shriver (1989). Briefly, the standard deviation of the data was derived from the residual in the fit assuming that all the points in the T_i curve have the same standard deviation. Next the fitted values of A and T_i were assumed to be the best estimates of the "true" values for these parameters, and simulated data sets were generated. These data sets were synthesized by a Gaussian random number generator which varied the points in the T_i curve within the standard deviation calculated above, producing y' values centered about $y = A \exp(-t/T_i)$. The same number of y' values were generated as experimental data points with each y' value corresponding to a time point that was actually obtained experimentally. The distribution of each of the parameters obtained from fits of the synthetic data sets are then used as an estimate of the goodness of fit. In the present study 250 data sets per T_i curve were generated. Figure 2 illustrates T_1 and T_2 data obtained for several residues as well as the best fits of the data. To estimate the error in NOE values, the standard deviation in baseline noise (σ) was determined for each spectrum and expanded into a standard deviation in volume given by

$$\Delta V = \sigma \sqrt{nk}$$

where n is the number of points in the f_1 dimension and k is the number of points in the f_2 dimension of a typical peak at

Table I: Relaxation Parameters Measured for the Leucine Methyl Carbons of Liganded and Unliganded SNase

carbon	liganded SNase						unliganded SNase ^b					
	T ₁ ^a	error	T ₂ ^a	error	NOE	error ^c	T ₁ ^a	error	T ₂ ^a	error	NOE	error ^c
L7 δ1	0.365	0.008	0.101	0.006	2.49	0.01	0.403	0.008	0.126	0.006	2.48	0.01
δ2	0.345	0.006	0.116	0.003	2.52	0.02	0.358	0.006	0.111	0.005	2.82	0.02
L14 δ1	0.316	0.008	0.072	0.002	2.83	0.02	0.293	0.007	0.070	0.003	2.85	0.03
δ2	0.463	0.009	0.093	0.005	2.89	0.02	0.496	0.009	0.095	0.003	2.90	0.03
L25 δ1	0.769	0.020	0.085	0.002	2.37	0.02	0.770	0.023	0.095	0.006	2.64	0.02
δ2	0.437	0.010	0.079	0.002	2.40	0.02	0.406	0.012	0.075	0.003	2.65	0.02
L36 δ1	0.249	0.003	0.097	0.003	2.49	0.02						
δ2	0.421	0.011	0.116	0.002	2.55	0.02	0.418	0.013	0.144	0.005	2.53	0.02
L37 δ1	0.206	0.005	0.056	0.003	2.44	0.02	0.285	0.005	0.083	0.002	2.60	0.03
δ2	0.278	0.004	0.074	0.002	2.66	0.02	0.370	0.013	0.099	0.002	2.46	0.02
L38 δ1	0.669	0.010	0.100	0.004	2.35	0.02	0.462	0.009	0.122	0.007	2.59	0.02
δ2	0.587	0.007	0.112	0.004	2.48	0.02	0.567	0.007	0.156	0.006	2.55	0.02
L89 δ1	0.393	0.007	0.077	0.002	2.52	0.02	0.397	0.016	0.098	0.002	2.41	0.02
δ2	1.191	0.020	0.082	0.004	1.87	0.01	0.928	0.020	0.111	0.005	2.01	0.02
L103 δ1	0.273	0.005	0.067	0.003	2.75	0.02	0.228	0.005	0.074	0.003	2.25	0.02
δ2	0.415	0.007	0.075	0.003	2.98	0.03						
L108 δ1	0.492	0.012	0.086	0.003	2.55	0.02	0.411	0.009	0.084	0.004	2.68	0.02
δ2	0.528	0.007	0.082	0.002	2.66	0.02	0.450	0.010	0.083	0.004	2.37	0.02
L125 δ1	0.361	0.006	0.111	0.003	2.62	0.02	0.339	0.007	0.146	0.009	2.95	0.03
δ2	0.599	0.010	0.144	0.005	2.54	0.02	0.621	0.009	0.166	0.004	2.96	0.03
L137 δ1	0.436	0.008	0.116	0.002	2.52	0.02	0.443	0.013	0.130	0.009	2.56	0.02
δ2	0.453	0.010	0.104	0.005	2.45	0.02	0.456	0.007	0.111	0.009	2.50	0.02

^aIn seconds. ^bSignals of L36 δ1 and L103 δ2 are coincident in the spectrum of unliganded SNase. ^cBased on root-mean-square noise in each spectrum.

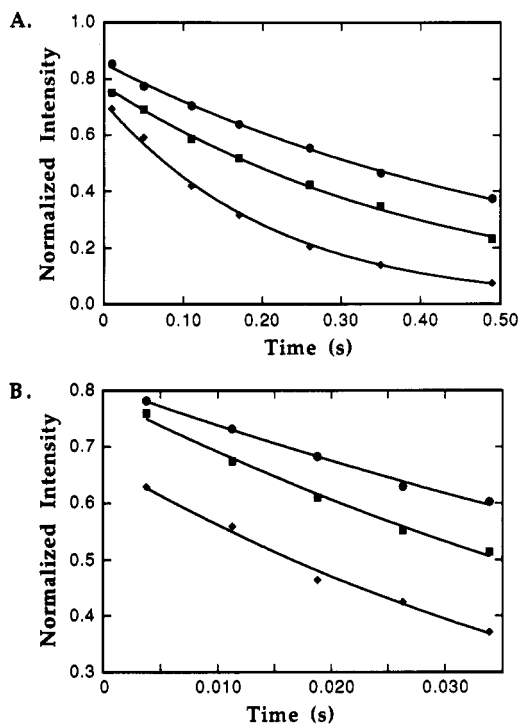


FIGURE 2: Experimental ¹³C relaxation data of selected residues of liganded SNase. Intensities are normalized to the largest peak in each set of spectra. The solid curves are single-exponential fits of the data. (A) T₁ and (B) T₂ data of (●) Leu-38, (■) Leu-103, and (◆) Leu-37.

the baseline. The error associated with the NOE value for peak *j* is then given by

$$\epsilon_j = \left(\frac{V_{A_j}}{V_{B_j}} \right) \sqrt{\left(\frac{\Delta V_A}{V_{A_j}} \right)^2 + \left(\frac{\Delta V_B}{V_{B_j}} \right)^2}$$

where V_{A_j} and V_{B_j} denote the volume of peak *j* in the presence and absence of NOE enhancement, respectively, and ΔV_A and ΔV_B denote the standard deviations in volume for the spectra recorded in the presence and absence of NOE enhancement, respectively. Table I lists values for T₁, T₂, and NOE and

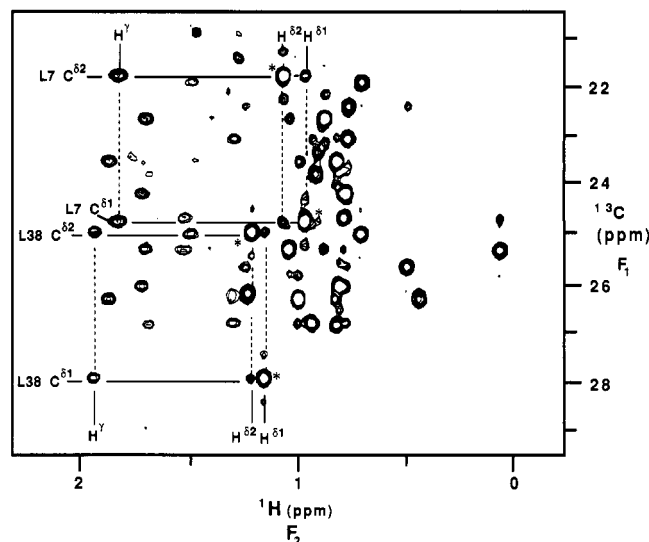


FIGURE 3: HMQC-RELAY spectrum of liganded SNase labeled with [5,5'-¹³C₂]leucine. Methyl carbon/methyl proton connectivities of Leu 7 and Leu 38 are identified with asterisks, and RELAY connectivities linking the methyl and γ-protons are joined by the solid horizontal lines. The vertical dotted lines link the two sets of connectivities found for Leu 7 and Leu 38. The remaining nine pairs of RELAY connectivity sets are identified in similar fashion. Note that weak doublets (parallel to F₁) flank the most intense methyl carbon/methyl proton cross-peaks, because the imperfect 180° pulse applied during *t*₁ evolution does not completely decouple the methyl protons from the methyl carbon.

associated errors for each leucine C^δ of SNase in the presence and absence of ligands (Ca²⁺ and pdTp).

RESULTS

Assignments of the Leucine Methyl Protons and Carbons. The chemical shifts of the 22 leucine methyl carbons were initially identified in [¹H-¹³C]HMQC and HMQC-RELAY (Figure 3) spectra of liganded SNase (the SNase/pdTp/Ca²⁺ ternary complex). The relay connectivities, linking each pair of methyl protons to their associated γ-proton and to one another, immediately established the spin system identifications of the γ-protons and the δ-protons and the δ-carbons of each

$= \sigma_{33} - \sigma_{11} = 25$ ppm (Spiess, 1978), the contributions of CSA to the T_1 and T_2 relaxation rates are over 20 times smaller than the dipolar contributions in the case of a methyl group, having a rotational correlation time about the 3-fold symmetry axis of ca. 30 ps, attached to a macromolecule tumbling with a correlation time of 9 ns. Moreover, cross-correlation effects between ^1H - ^{13}C dipolar and ^{13}C CSA interactions are effectively suppressed by the pulse sequences applied (Kay et al., 1992a). The spin rotation contribution to the methyl carbon relaxation in SNase is also negligible. It has been shown (Spiess et al., 1973) that the SR contribution to the spin lattice relaxation of the methyl carbon of toluene at 60 °C is less than 0.05 s^{-1} . This represents the upper limit of the contribution of SR to methyl carbon relaxation in SNase since there is essentially no barrier to methyl rotation in toluene. In SNase the calculated and measured dipolar relaxation rates of the leucine methyl carbons are greater than 0.8 s^{-1} , over 15 times larger than the maximum possible contribution from the SR relaxation mechanism.

The T_1 relaxation data show essentially no deviation from single-exponential decay, strongly indicating that cross-correlation does not significantly affect the T_1 and NOE determinations (Werbellow & Grant, 1977). This conclusion was confirmed by extensive calculations (Kay & Torchia, 1991) of the T_1 and NOE values, including the effects of cross-correlation, (Werbellow & Grant, 1977) using the Woessner model in which the internal methyl rotation is characterized by a three-site jump about its symmetry axis (Woessner, 1962) to simulate the overall and internal motions of the leucine methyl groups in SNase. Use of the three-site jump version of the Woessner model rather than the free diffusion version is substantiated by neutron diffraction studies of L-alanine (Lehmann et al., 1972) and L-valine (Koetzle et al., 1974), in which three discrete positions are observed for the methyl deuterons, rather than a ring of intensity as would be observed for the case of free diffusion about the 3-fold symmetry axis. The fact that ^1H - ^{13}C dipolar cross-correlation does not significantly affect the measured T_1 and NOE values is due (a) to a fortuitous cancellation of terms that comprise the cross-correlation spectral density functions and (b) to spin flips between protons directly attached to the heteroatom and neighboring proton spins. Rapid proton spin flips effectively average out the differential longitudinal relaxation rates of individual ^{13}C transitions (Kay & Torchia, 1991; Kay et al., 1992b). In contrast, the T_2 calculations based upon the Woessner model (Kay & Torchia, 1991) predict (a) that decay of transverse magnetization is biexponential, e.g., if $\tau_m \rightarrow \infty$ and $\tau_c \rightarrow 0$, the limiting slope at $t \rightarrow 0$ is 3-fold larger than the limiting slope at $t \rightarrow \infty$, where τ_m is the overall correlation time, τ_c is the effective correlation time (Lipari & Szabo, 1982a,b), and t is the relaxation delay, and (b) that the degree of biexponential decay of transverse magnetization depends critically upon the model of motion that is used and upon the size of contributions to the relaxation process made by protons that are close to the methyl groups. Because the transverse decay rates of the fastest decaying ^{13}C transitions are faster than the rate of proton spin flips, the spin flips do not average out the differential ^{13}C relaxation in an efficient manner. Partial averaging can be achieved by the application of ^1H 125° pulses at the height of the spin echo in the CPMG interval indicated in Figure 2B at a rate that is fast compared to the fastest decaying component of ^{13}C magnetization (Kay et al., 1992a).

The analysis of the relaxation data in terms of the minimum number of unique motional parameters is most easily achieved

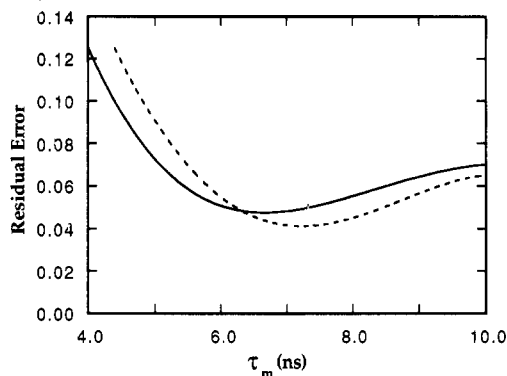


FIGURE 5: Residual error $\{\chi^2/3N\}^{0.5}$, where χ^2 is defined in eq 5 and N is the number of C^δ carbons that are included in the summation, as a function of τ_m for SNase with (solid line) and without (dashed line) ligands.

using the formalism of Lipari and Szabo (1982a,b) where $J(\omega_i)$ is expressed according to

$$J(\omega_i) = \frac{2}{5} \left[\frac{S^2 \tau_m}{1 + (\omega_i \tau_m)^2} + \frac{(1 - S^2) \tau_c}{1 + (\omega_i \tau_c)^2} \right] \quad (4)$$

with $\tau^{-1} = \tau_m^{-1} + \tau_c^{-1}$, where τ_m is the isotropic tumbling time and τ_c is an effective correlation time describing the rapid internal motions. Our initial approach to the analysis of the relaxation data was to fit the T_1 , T_2 , and NOE data for each Leu C^δ carbon simultaneously using values of τ_m ranging from 1 to 15 ns in steps of 0.1 ns. In this way best values of $S^2(j)$ and $\tau_c(j)$ were calculated for each C^δ carbon (j) as a function of τ_m . In addition, a residual χ^2 was calculated (Dellwo & Wand, 1989) according to

$$\chi^2 = \sum \left[\left(\frac{T_1^e - T_1^c}{T_1^e} \right)^2 + \left(\frac{T_2^e - T_2^c}{T_2^e} \right)^2 + \left(\frac{\text{NOE}^e - \text{NOE}^c}{\text{NOE}^e} \right)^2 \right] \quad (5)$$

where T_i^e and T_i^c are the experimental and calculated values of T_i and NOE^e and NOE^c refer to the experimental and calculated values for the NOE. In eq 5 the summation runs over all the C^δ carbons. The best values of τ_m , $S^2(j)$, and $\tau_c(j)$ are chosen as the values which minimize χ^2 . Figure 5 shows a plot of χ^2 as a function of τ_m . As expected, the overall correlation time of SNase with and without ligands is approximately the same, with a minimum in χ^2 measured at $\tau_m \sim 6.6$ ns for liganded SNase and $\tau_m \sim 7.2$ ns for unliganded SNase. The values of τ_m calculated using this approach are significantly smaller than the value of ~ 9 ns obtained from ^{15}N T_1 , T_2 , and NOE relaxation measurements reported previously for SNase complexed with pTp and Ca^{2+} (Kay et al., 1989). In addition, ^{13}C T_1 , T_2 , and NOE measurements of SNase labeled in the C^α position of proline residues indicated that the overall correlation time of the protein was 8.6 ns under conditions identical to those used for measuring the leucine C^δ relaxation parameters. A close inspection of the fits of the data revealed that while experimental T_1 and T_2 values were reproduced well, the NOE values predicted on the basis of the best values of τ_m , $S^2(j)$, and $\tau_c(j)$ were in general larger than the experimental NOE values by as much as 10–15%. These deviations are much larger than what would be predicted on the basis of the experimental error, since NOE error values of $\sim 1\%$ were obtained on the basis of the root-mean-square deviation of baseline noise.

The discrepancies outlined above suggest that the model used to fit the relaxation data (see eq 4) of the leucine C^δ

Table III: Effective Correlation Times^a Obtained for Fast Internal Motions, τ_f , and the Order Parameters,^b S_s^2 and S_{LZ}^2 , of Leucine Methyl Carbons

carbon	liganded SNase					unliganded SNase				
	τ_f	S_s^2	error ^c	S_{LZ}^2	error ^c	τ_f	S_s^2	error ^c	S_{LZ}^2	error ^c
L7 δ_1	0.032	0.591	0.048	0.631	0.060	0.026	0.449	0.031	0.478	0.038
δ_2	0.034	0.466	0.022	0.479	0.023	0.047	0.518	0.040	0.524	0.031
L14 δ_1	0.053	0.890	0.028	0.885	0.034	0.058	0.887	0.036	0.897	0.043
δ_2	0.040	0.727	0.048	0.706	0.052	0.037	0.717	0.028	0.707	0.023
L25 δ_1	0.014	0.891	0.054	0.878	0.023	0.022	0.777	0.052	0.754	0.056
δ_2	0.029	0.815	0.028	0.906	0.025	0.035	0.910	0.039	0.898	0.041
L36 δ_1	0.053	0.463	0.036	0.527	0.023					
δ_2	0.026	0.516	0.013	0.533	0.015	0.024	0.369	0.023	0.379	0.025
L37 δ_1	0.083	0.958	0.030	0.955	0.028	0.049	0.640	0.088	0.725	0.028
δ_2	0.054	0.819	0.051	0.840	0.034	0.032	0.601	0.021	0.629	0.014
L38 δ_1	0.014	0.697	0.061	0.755	0.029	0.023	0.502	0.037	0.506	0.042
δ_2	0.016	0.602	0.025	0.612	0.028	0.015	0.381	0.023	0.401	0.022
L89 δ_1	0.034	0.840	0.031	0.881	0.024	0.029	0.577	0.085	0.667	0.021
δ_2	0.005	0.916	0.030	0.980	0.014	0.005	0.654	0.037	0.792	0.023
L103 δ_1	0.060	0.931	0.039	0.913	0.044	0.065	0.688	0.037	0.806	0.050
δ_2	0.040	0.881	0.038	0.878	0.029					
L108 δ_1	0.025	0.806	0.051	0.803	0.036	0.035	0.787	0.057	0.788	0.040
δ_2	0.028	0.884	0.036	0.855	0.027	0.027	0.757	0.046	0.840	0.033
L125 δ_1	0.034	0.516	0.018	0.523	0.022	0.059	0.331	0.041	0.319	0.038
δ_2	0.014	0.441	0.018	0.451	0.022	0.038	0.373	0.012	0.364	0.014
L137 δ_1	0.025	0.522	0.011	0.544	0.011	0.023	0.443	0.050	0.491	0.045
δ_2	0.024	0.612	0.045	0.630	0.027	0.024	0.570	0.056	0.640	0.048

^aIn nanoseconds. ^bThe values of S_f^2 are assumed to equal 0.111, and τ_m is 8.5 ns. The slow motion order parameter obtained using the Lipari-Szabo analysis, S_{LZ}^2 (eq 3 divided by 0.111), is listed to allow comparison with S_s^2 . ^cPrecision limits were determined using the Monte Carlo procedure described in the text. The values of τ_s typically lie in the range of 0.2–2 ns but are not listed because they have very large uncertainties.

groups is not appropriate. As has been described previously (Kay et al., 1989), the assumption of isotropic motion for SNase is well founded since the principle components of the inertia tensor of the molecule are in the ratio of 1.0:1.3:1.4; additionally, values of τ_m calculated at each ¹⁵N position in the molecule were found to be very similar. A likely reason for the poor fitting of the NOE data as well as the calculated low value of τ_m is the assumption that the internal dynamics of the methyl groups can be described completely in terms of a single effective correlation time. We therefore assume that, in addition to rapid methyl jumps about the C ^{γ} -C ^{δ} bond, an additional internal motion corresponding to reorientation of the C ^{γ} -C ^{δ} bond on a time scale intermediate between the methyl jump rate and the overall tumbling rate of the protein is present. To obtain the simplest description consistent with this model, we have chosen to fit our data using a spectral density function of the following form

$$J(\omega) = \frac{2}{5} \left[\frac{S^2 \tau_m}{1 + (\omega \tau_m)^2} + \frac{(1 - S_f^2) \tau_1}{1 + (\omega \tau_1)^2} + \frac{S_f^2 (1 - S_s^2) \tau_2}{1 + (\omega \tau_2)^2} \right] \quad (6)$$

where S_f and S_s are the order parameters describing the fast and slow motions, respectively, $S^2 = S_f^2 S_s^2$, $\tau_1^{-1} = \tau_m^{-1} + \tau_f^{-1}$, $\tau_2^{-1} = \tau_m^{-1} + \tau_s^{-1}$, and τ_f and τ_s are the effective correlation times for the fast and slow motions, respectively (Clare et al., 1990b,c). Inspection of eq 6 reveals that a fit of the data requires four parameters for each carbon: S_f^2 , S_s^2 , τ_s , and τ_f . In addition, a single global parameter for the overall correlation time of the protein, τ_m , is needed.

The situation is simplified somewhat by noting that in the case of a methyl group executing rapid jumps between three equilibrium positions about its 3-fold axis (the C ^{γ} -C ^{δ} bond axis), the rate of methyl rotation is characterized by a single correlation time, τ_f , and a generalized order parameter, S_f , which is given by

$$S_f = \frac{(3 \cos^2 \beta - 1)}{2} \quad (7)$$

where β is the angle between the ¹³C-¹H bond vector and the rotation axis. Thus, S_f^2 reduces to 0.111 for the case of perfect tetrahedral geometry. Finally, assuming perfect tetrahedral geometry, and using a value for τ_m of 8.5 ns, based on ¹⁵N relaxation studies (Kay et al., 1989, 1992b) as well as on ¹³C relaxation measurements of the C ^{α} carbon in Pro residues discussed previously, the determination of S_s^2 , τ_s , and τ_f is achieved from conjugate gradient minimization of eq 5 for each residue. Using this extended model describing the methyl group dynamics, one obtains values for T_1 , T_2 , and NOE^c that are in good agreement with experiment. The values of S_s^2 , τ_s , and τ_f for each site determined with the above approach are listed in Table III.

The sensitivity of S_f^2 to methyl group geometry is the limiting factor in our determination of S_s^2 for the [¹³C _{δ}]Leu sites studied. Single-crystal neutron diffraction studies on L-alanine (Lehmann et al., 1972) and L-valine (Koetzle et al., 1974) have elucidated methyl group structures that are slightly distorted from ideal tetrahedral geometry. The reported geometry for the L-alanine methyl group is relatively symmetric and results in a theoretical S_f^2 value of 0.104. Both methyl groups in the reported L-valine structure exhibit a larger deviation from ideal tetrahedral geometry and yield S_f^2 values of 0.085 and 0.090 for the γ^1 and γ^2 methyl groups, respectively. If a value of 0.090 for S_f^2 were assumed, the S_s^2 values listed in Table III would be increased by ~20%, resulting in a number of sites having physically unreasonable S_s^2 values of >1.00. Furthermore, inherent in the reported structures of methyl groups in amino acid single crystals are the effects of strong crystal packing forces associated with the zwitterionic nature of the compounds which may slightly affect the structure of the methyl group. For these reasons, we have chosen to evaluate the dynamics of the leucine methyl groups in SNase on the basis of ideal tetrahedral geometry ($S_f^2 = 0.111$), while recognizing that the effects of nonideal geometry may lead to variations in the resulting S_s^2 values of 10–20%.

The X-ray temperature factor (Loll & Lattman, 1989; Hynes & Fox, 1991) is plotted against the corresponding value of S_s^2 for each leucine δ -carbon in liganded and unliganded

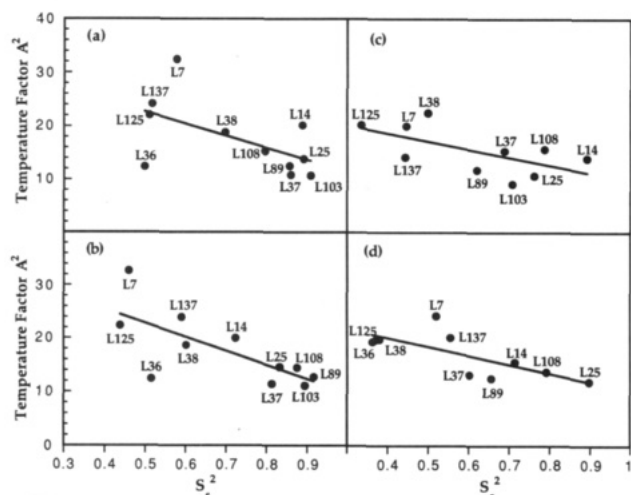


FIGURE 6: Plot of S_s^2 against X-ray temperature factors for liganded SNase (a and b), and unliganded SNase (c and d). Plots a and c correspond to δ_1 carbons, and plots b and d to δ_2 carbons. The straight lines are the least-squares fits to the data. The linear fit is chosen as a simple means of indicating the trends of the data.

SNase in Figure 6a–d. While the correlation between the temperature factors and order parameters is reasonably good, it is not perfect. This result is not surprising when one considers that the temperature factors arise from static disorder and from atomic displacements taking place on a time scale ranging from at least 10^{-13} to 10^4 s, whereas the order parameters derived from NMR relaxation measurements are sensitive only to internal motions having correlation times less than τ_m . An interesting feature of the leucine temperature factors is that, in a given residue, the methyl carbon temperature factors do not differ significantly from the temperature factors of the leucine backbone atoms. This result is apparently due to the fact that all leucine methyl groups are buried in the closely packed interior of crystalline SNase. In contrast, the residues at the protein surface have side chain atom temperature factors that are significantly larger than their backbone atom temperature factors. For liganded SNase in solution, the order parameters determined for the leucine methyl carbons divide the leucine side chains into two groups, “flexible” ($0.44 < S_s^2 < 0.71$) and “rigid” ($0.80 < S_s^2 < 0.92$). For the rigid sites (L14, L25, L37, L89, L103, and L108), the side chain order parameters are approximately the same as the corresponding backbone amide values ($0.82 < S_s^2 < 0.92$) derived from measurements of ^{15}N relaxation parameters (Kay et al., 1989). However, for the flexible sites (L7, L36, L38, L125, and L137) the values of leucine methyl order parameters are much smaller than the corresponding values of the leucine backbone amide order parameters, $0.87 < S_s^2 < 0.93$ (Kay et al., 1989), suggesting that in solution there is significant internal motion of specific buried leucine side chains of SNase.

Comparison of leucine methyl order parameters determined for liganded and unliganded SNase yields information concerning the effect of ligand binding on dynamics of side chains distributed throughout the protein. The locations of the 11 leucine residues in SNase are shown in Figure 7, with the labeled C^δ atoms depicted as either open or solid spheres. Because the order parameters of the δ_1 and δ_2 carbons of each leucine side chain are nearly the same, the average value of each pair is used. The average order parameter for each leucine side chain in the liganded and unliganded forms of SNase is plotted in Figure 8. Six of the leucine side chains (L36, L37, L38, L89, L103, and L125) showed a significant difference in average order parameter (ΔS_s^2) between the

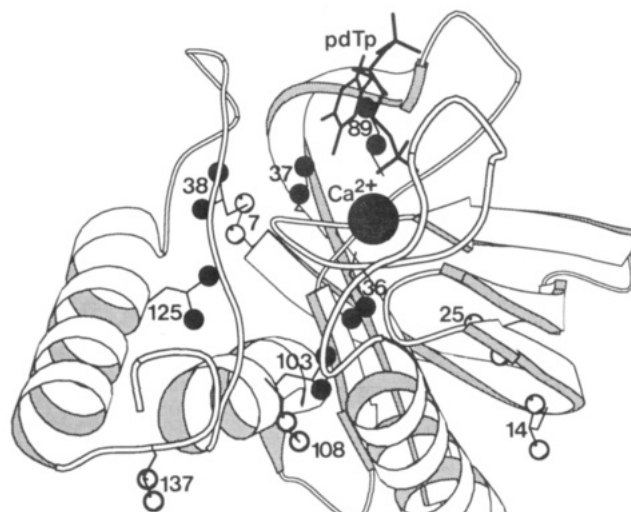


FIGURE 7: Structure of liganded SNase as derived from X-ray crystal coordinates (Hynes & Fox, 1991). The bonds within the 11 leucine side chains are shown as thin lines, with the $^{13}\text{C}_6$ atoms accentuated by spheres. Leucine sites which show a substantial increase in S_s^2 upon ligand binding are shown as solid spheres, and those that show little change are shown as open spheres. The bonds within the pdTp ligand are shown as heavy lines, and the Ca^{2+} ligand as a large stippled sphere.

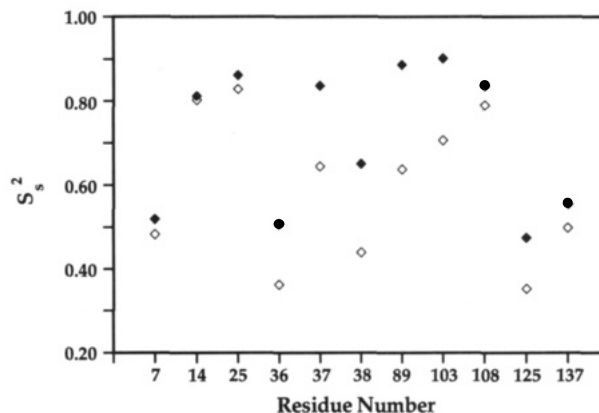


FIGURE 8: Plot of the average S_s^2 for each δ_1, δ_2 pair in the presence (◆) and absence (◇) of ligands (Ca^{2+} and pdTp) for each residue. All sites show an increase in average S_s^2 upon ligand binding, and sites nearest to the binding site show the largest increase.

liganded and unliganded forms. These residues are shown as solid spheres in Figure 7. In all six cases, the order parameter for each pair of leucine δ -carbons increased by more than 29% upon ligand binding, indicating a substantial reduction of amplitude of motion in the liganded form. According to the X-ray crystal structure of liganded SNase (Loll & Lattman, 1989), each of the C^δ atoms for these six side chains is within 10 \AA of either the Ca^{2+} atom or at least one of the heavy atoms comprising the pdTp, while the C^δ atoms of the remaining five leucines are not. Furthermore, those sites which showed the largest increase in S_s^2 upon ligand binding (L37, L38, and L89) are closest to the active site, all having a separation of less than 6.5 \AA from at least one of the pdTp heavy atoms. Thus, significant differences in dynamics of leucine side chains between the liganded and unliganded forms are observed, and a strong correlation is found between ΔS_s^2 and distance between leucine methyl carbons and ligand atoms in the active site (Loll & Lattman, 1989). The X-ray crystal structures for the liganded (Loll & Lattman, 1989) and unliganded (Hynes & Fox, 1991) forms of SNase show that the size and

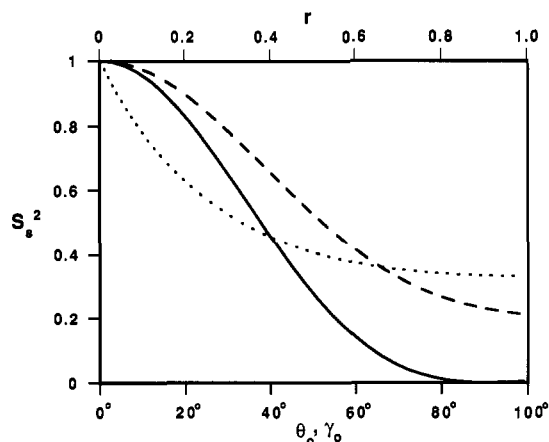


FIGURE 9: Plots of S_s^2 as a function of θ_0 , γ_0 , and r for the cone (solid line), restricted diffusion (dashed line), and two-site jump (dotted line) models, respectively, calculated using eq 8–10.

shape of the active site remain relatively unchanged upon ligand binding. Mobile solvent molecules and a few side chains are displaced by the Ca^{2+} and pdTp , and the disordered Ω loop has a different average conformation. However, the unliganded molecule undergoes thermal unfolding at a temperature 15–20 °C lower than liganded SNase. Also, in liganded SNase the exchange rates of the most slowly exchanging amides are 2–3 orders of magnitude smaller than in unliganded SNase (Baldissari and Torchia, unpublished observations). These observations which attest to the greater stability of the liganded protein are consistent with the differences in dynamics of the leucine side chains observed for the two forms of the enzyme.

In order to further characterize the flexibility of the protein, we consider three plausible models of internal motion of the leucine side chains that yield order parameters that are in agreement with the experimental values of S_s^2 .

The Cone Model. If the $\text{C}^\gamma\text{--C}^\delta$ bond axis diffuses in a cone of semiangle θ_0 , S_s^2 is given by

$$S_s^2 = \left[\frac{\cos \theta_0 (1 + \cos \theta_0)}{2} \right]^2 \quad (8)$$

and S_s^2 is plotted as a function of θ_0 in Figure 9.

The Restricted Diffusion Model. If the leucine side chain undergoes rotational diffusion about the $\text{C}^\beta\text{--C}^\gamma$ bond axis through an angular range of $\pm\gamma_0$, S_s^2 is given by (Lipari & Szabo, 1982b)

$$S_s^2 = \frac{1}{9} \left[1 + \frac{8 \sin^2 \gamma_0 (1 + 2 \cos^2 \gamma_0)}{3 \gamma_0^2} \right] \quad (9)$$

and S_s^2 is plotted as a function of γ_0 in Figure 9.

The Two-Site Jump Model. If the $\text{C}^\gamma\text{--C}^\delta$ bond axis abruptly changes its orientation by 109.5°, S_s^2 is given by

$$S_s^2 = 1 - \frac{8}{3} \left[\frac{r}{(1+r)^2} \right] \quad (10)$$

where $r = p_1/p_2$, and p_1 and p_2 are the relative populations of the two orientations of the bond axis. S_s^2 is plotted against r in Figure 9.

Our consideration of the two-site jump model is motivated by reports that the leucine side chain exists predominately in only two of the nine possible rotamer conformations ($\chi_1 = 300^\circ$, $\chi_2 = 180^\circ$; $\chi_1 = 180^\circ$, $\chi_2 = 60^\circ$) in crystals in peptides

Table IV: Values of S_s^2 and Corresponding Values of θ_0 , γ_0 , and r Derived from the Cone, Restricted Diffusion, and Two-Site Jump Models of Leucine Side Chain Motion, Respectively, for Flexible Sites in Liganded (L) and Unliganded (U) SNase

residue	S_s^2	θ_0 (deg)	γ_0 (deg)	r
L7 (L)	0.53	36	50	0.30
(U)	0.48	39	54	0.36
L36 (L)	0.49	38	53	0.35
(U)	0.37	45	65	0.62
L37 (L)	0.89	16	21	0.05
(U)	0.62	32	43	0.21
L38 (L)	0.65	30	41	0.18
(U)	0.44	41	58	0.43
L89 (L)	0.88	17	22	0.05
(U)	0.62	32	43	0.21
L103 (L)	0.91	14	19	0.04
(U)	0.69	28	38	0.16
L125 (L)	0.48	39	54	0.36
(U)	0.35	46	67	0.73
L137 (L)	0.57	34	47	0.25
(U)	0.50	38	52	0.33

(Benedetti, 1977) and proteins (Janin et al., 1978). ^2H NMR studies have provided strong evidence that these two side chain conformations convert rapidly, $\tau < 10^{-7}$ s, in collagen (Batchelder et al., 1982) and in the fd coat protein (Colnago et al., 1987).

The order parameters of the flexible ($S_s^2 < 0.7$) leucine side chains in liganded (L7, L36, L38, L125, and L137) and unliganded (L7, L36, L37, L89, L103, L125, and L137) SNase are used to estimate the range of motion of these buried sites for the three models of motion. Again, the average value of each δ_1, δ_2 pair is used. These order parameters together with eqs 8–10 yield the values of θ_0 , γ_0 , and r for each side chain. Examination of Table IV shows that the internal motions of the flexible leucine side chains have substantial angular amplitudes in the case of both the cone and restricted diffusion models. Alternatively, in the two-site jump model where the angular amplitude is fixed, Table IV shows that the minor conformation for these side chains is always significantly populated. Therefore, one finds that all five flexible leucine side chains in liganded SNase and all eight in unliganded SNase undergo substantial internal motions in the case of each of the models considered. Furthermore, for the six side chains which show a substantial increase in S_s^2 upon ligand binding, changes in amplitude of as much as 50% are observed. We note that our analysis has not included the possible contributions of chemical exchange and CSA to the measured value of T_2 . The neglect of either of these contributions, if they are in fact significant, causes S_s^2 to be overestimated and results in an underestimation of the degree of internal motion.

The presence of large amplitude internal motions of the leucine side chains in SNase is interesting because nearly all 11 side chains are buried within the protein interior (Loll & Lattman, 1989) and the only methyl groups with significant solvent exposure are $\text{L14C}^{\delta 1}$ and $\text{L137C}^{\delta 1}$. Also, the temperature factors of the leucine methyl carbons are less than or equal to the temperature factors of the motionally restricted leucine backbone atoms (Loll & Lattman, 1989). These results suggest that motions of interior side chains that are observed herein are hindered by formation of the crystal lattice, perhaps because such motions cause small perturbations in the overall shape of the protein that cannot be accommodated without distorting the lattice.

We have noted in discussing the NMR signal assignments that the relative intensities of the NOE connectivities involving the methyl protons and various backbone and buried side chain protons are in qualitative agreement with internuclear distances

obtained from the crystal structures of liganded and unliganded SNase. It may appear paradoxical that this statement applies to the methyl protons of leucine residues that have flexible side chains. However, it has been shown that if protons are separated by several bonds and do not have highly correlated motions, then the NOE intensities calculated in the presence of rapid internal motions do not greatly differ from NOE intensities calculated with the protons fixed at their average positions (LeMaster et al., 1988). This result is a consequence of the fact that effects upon the NOE of angular and radial fluctuations of internuclear vectors tend to compensate one another. It seems reasonable that the positions of the leucine methyl carbons in the crystalline state are the averages of the distribution of positions sampled in the solution state. A computer simulation of SNase molecular dynamics might provide useful insights into the reasons for the variation of the leucine order parameters and for the apparent differences in flexibility of the side chains in the solution and crystalline states.

Studies of methyl carbons of assigned hydrophobic side chains have been reported for BPTI (Richarz et al., 1980) and myoglobin (Jones et al., 1976). The order parameters obtained for I18, I19, L6, and M52 in BPTI and RCAM-BPTI, after factoring out the contribution due to methyl rotation (assuming tetrahedral geometry), are slightly lower than the range observed for the Leu methyl carbons of SNase (Table III). Hence, it appears that larger amplitude side chain motions occur in the hydrophobic domains of BPTI than in SNase.

In the case of myoglobin, the order parameters obtained for the methyl carbons of M55 and M131 (Jones et al., 1976) are in the ranges of methyl order parameters observed for BPTI and for SNase. In addition, order parameters have been obtained for the δ -carbons of seven Ile (not assigned) residues in myoglobin (Wittebort et al., 1979). In contrast with the methionine order parameters, the value of S_{α}^2 obtained for every myoglobin Ile methyl carbon is greater than the largest SNase Leu order parameter listed in Table III. It has been noted that some of the myoglobin Ile order parameters may be in error because interpretation of the data is complicated by possible paramagnetic contributions to the relaxation mechanism.

Because of the limited experimental data currently available, it is not known if motions of large hydrophobic residues, similar to the large amplitude motions observed in SNase and in BPTI, generally occur in proteins. It is clear that the high sensitivity afforded by modern proton-detected heteronuclear two-dimensional NMR techniques makes it feasible to measure the relaxation parameters of a large number of assigned backbone and side chain atoms in proteins. Such data will provide important dynamic information that will complement the wealth of structural information available from X-ray and NMR studies. While it is essential to know the three-dimensional structure of a protein in order to understand its function, it is equally important to have information, provided by relaxation studies, about the amplitude and time scale of structural fluctuations.

ACKNOWLEDGMENTS

We thank Professor David Shortle for the plasmid encoding for the production of SNase, Professor Robert Fox for the X-ray coordinates of unliganded SNase, Rolf Tschudin for expert technical support, and New Methods Research (Syracuse, NY) for providing a copy of their software.

SUPPLEMENTARY MATERIAL AVAILABLE

A detailed description of the synthesis of D,L -[5,5'- $^{13}C_2$]-

leucine (3 pages). Ordering information is given on any current masthead page.

REFERENCES

- Abragam, A. (1961) in *The Principles of Nuclear Magnetism* (Marshall, W. C., & Wilkinson, D. H., Eds.) pp 289-305, Clarendon Press, Oxford.
- Baldisseri, D. M., Pelton, J. G., Sparks, S. W., & Torchia, D. A. (1991) *FEBS Lett.* 281, 33.
- Batchelder, L. S., Sullivan, C. E., Jelinski, L. W., & Torchia, D. A. (1982) *Proc. Natl. Acad. Sci. U.S.A.* 79, 386.
- Bax, A., & Weiss, M. A. (1987) *J. Magn. Reson.* 71, 571.
- Bax, A., Clore, G. M., & Gronenborn, A. M. (1990a) *J. Magn. Reson.* 88, 425.
- Bax, A., Ikura, I., Kay, L. E., Torchia, D. A., & Tschudin, R. (1990b) *J. Magn. Reson.* 86, 304.
- Bendall, M. R., Pegg, D. T., Doddrell, D. M., & Field, J. (1983) *J. Magn. Reson.* 51, 520.
- Benedetti, C. (1977) in *Proceedings of the Fifth American Peptide Symposium* (Goodman, M., & Meienhofer, J., Eds.) pp 257-274, Wiley, New York.
- Carr, H. Y., & Purcell, E. M. (1954) *Phys. Rev.* 94, 630.
- Clore, G. M., Bax, A., Driscoll, P. C., Wingfield, P. T., & Gronenborn, A. M. (1990a) *Biochemistry* 29, 8172.
- Clore, G. M., Szabo, A., Bax, A., Kay, L. E., Driscoll, P. C., & Gronenborn, A. M. (1990b) *J. Am. Chem. Soc.* 112, 4989.
- Clore, G. M., Driscoll, P. C., Wingfield, P. T., & Gronenborn, A. M. (1990c) *Biochemistry* 29, 7387.
- Colnago, L. A., Valentine, K. G., & Opella, S. J. (1987) *Biochemistry* 26, 847.
- Dellwo, M. J., & Wand, A. J. (1989) *J. Am. Chem. Soc.* 111, 4571.
- Doddrell, D. M., Pegg, D. T., & Bendall, M. R. (1982) *J. Magn. Reson.* 48, 323.
- Frey, M. N., Koetzle, T. F., Lehmann, M. S., & Hamilton, W. C. (1973) *J. Chem. Phys.* 59, 915.
- Hynes, T. R., & Fox, R. O. (1991) *Proteins: Struct., Funct., Genet.* 10, 92.
- Ikura, M., Kay, L. E., & Bax, A. (1990) *Biochemistry* 29, 4659.
- Janin, J., Wodak, S., Levitt, M., & Maigret, B. (1978) *J. Mol. Biol.* 125, 357.
- Jones, W. C., Rothgeb, T. M., & Gurd, F. R. N. (1976) *J. Biol. Chem.* 251, 7452.
- Kamath, U., & Shriver, J. W. (1989) *J. Biol. Chem.* 264, 5586.
- Kay, L. E., & Torchia, D. A. (1991) *J. Magn. Reson.* 95, 536.
- Kay, L. E., Torchia, D. A., & Bax, A. (1989) *Biochemistry* 28, 8972.
- Kay, L. E., Clore, G. M., Bax, A., & Gronenborn, A. M. (1990a) *Science* 249, 411.
- Kay, L. E., Ikura, M., & Bax, A. (1990b) *J. Am. Chem. Soc.* 112, 888.
- Kay, L. E., Bull, T. E., Nicholson, L. K., Griesinger, C., Schwalbe, H., Bax, A., & Torchia, D. A. (1992a) *J. Magn. Reson.* (in press).
- Kay, L. E., Nicholson, L. K., Delaglio, F., Bax, A., & Torchia, D. A. (1992b) *J. Magn. Reson.* 97, 359.
- Koetzle, T. F., Golic, L., Lehmann, M. S., Verbist, J. J., & Hamilton, W. C. (1974) *J. Chem. Phys.* 60, 4690.
- Lehmann, M. S., Koetzle, T. F., & Hamilton, W. C. (1972) *J. Am. Chem. Soc.* 94, 2657.
- LeMaster, D. M., Kay, L. E., Brunger, A. T., & Prestegard, J. H. (1988) *FEBS Lett.* 236, 71.
- Lerner, L., & Bax, A. (1986) *J. Magn. Reson.* 69, 375.

- Lipari, G., & Szabo, A. (1982a) *J. Am. Chem. Soc.* 104, 4546.
 Lipari, G., & Szabo, A. (1982b) *J. Am. Chem. Soc.* 104, 4559.
 Loll, P. G., & Lattman, E. E. (1989) *Proteins: Struct., Funct., Genet.* 5, 1983.
 Marion, D., & Wüthrich, K. (1983) *Biochem. Biophys. Res. Commun.* 113, 967.
 Markley, J. L., Jorsley, W. J., & Klein, M. P. (1971) *J. Chem. Phys.* 55, 3604.
 McCain, D. C., Ulrich, E. L., & Markley, J. L. (1988) *J. Magn. Reson.* 80, 296.
 Meiboom, S., & Gill, D. (1958) *Rev. Sci. Instrum.* 29, 688.
 Neri, D., Szyperski, T., Otting, G., Seen, H., & Wüthrich, K. (1989) *Biochemistry* 28, 7510.
 Nirmala, N. R., & Wagner, G. (1988) *J. Am. Chem. Soc.* 110, 7557.
 Nirmala, N. R., & Wagner, G. (1989) *J. Magn. Reson.* 82, 659.
 Palmer, A. G., III, Rance, M., & Wright, P. E. (1991a) *J. Am. Chem. Soc.* 113, 4371.
 Palmer, A. G., III, Wright, P. E., & Rance, M. (1991b) *Chem. Phys. Lett.* 185, 41.
 Press, W. H., Flannery, B. P., Teukolsky, S. A., & Vetterling, W. T. (1988) in *Numerical Recipes in C*, pp 317-323, Cambridge University Press, Cambridge.
 Richarz, R., Nagayama, K., & Wüthrich, K. (1980) *Biochemistry* 19, 5189.
 Shaka, A. J., Keeler, J., & Freeman, R. (1983) *J. Magn. Reson.* 53, 313.
 Sklenar, V., Torchia, D. A., & Bax, A. (1987) *J. Magn. Reson.* 73, 375.
 Sparks, S. W., Cole, H. B. R., Torchia, D. A., & Young, P. E. (1989) *Chem. Scr.* 29A, 31.
 Spiess, H. W. (1978) *NMR: Basic Princ. Prog.* 15, 55.
 Spiess, H. W., Schweitzer, D., & Haebleren, U. (1973) *J. Magn. Reson.* 9, 444.
 Torchia, D. A., Sparks, S. W., & Bax, A. (1989a) *Biochemistry* 28, 5509.
 Torchia, D. A., Sparks, S. W., Young, P. E., & Bax, A. (1989b) *J. Am. Chem. Soc.* 111, 8315.
 Wang, J., LeMaster, D. M., & Markley, J. M. (1990a) *Biochemistry* 29, 88.
 Wang, J., Hinck, A. P., Loh, S. N., & Markley, J. M. (1990b) *Biochemistry* 29, 4242.
 Werbelow, L. G., & Grant, D. M. (1977) *Adv. Magn. Reson.* 9, 189.
 Wittebort, R. J., Rothgeb, T. M., Szabo, A., & Gurd, F. R. N. (1979) *Proc. Natl. Acad. Sci. U.S.A.* 76, 1059.
 Woessner, D. E. (1962) *J. Chem. Phys.* 36, 1.

¹H NMR and NOE Studies of the Purple Acid Phosphatases from Porcine Uterus and Bovine Spleen[†]

Zhigang Wang, Li-June Ming, and Lawrence Que, Jr.*

Department of Chemistry, University of Minnesota, Minneapolis, Minnesota 55455

John B. Vincent, Michael W. Crowder, and Bruce A. Averill

Department of Chemistry, University of Virginia, Charlottesville, Virginia 22901

Received January 23, 1992; Revised Manuscript Received April 2, 1992

ABSTRACT: The diiron active sites of the purple acid phosphatases from porcine uterus (also called uteroferrin, Uf) and bovine spleen (BSPAP) and their complexes with tungstate are compared by ¹H NMR and NOE techniques. The paramagnetically shifted features of the ¹H NMR spectrum of reduced BSPAP are similar to those of reduced Uf, while the spectra of the tungstate complexes are almost identical. These observations suggest that the two active sites are quite similar, in agreement with the >90% sequence homology found in the two enzymes. Nuclear Overhauser effect (NOE) experiments on the His N-H resonances show that the Fe(III)-His residue is N_c-coordinated, while the Fe(II)-His is H_β-coordinated in both enzymes. On the basis of the above NMR and NOE results, our previously proposed model for the dinuclear iron active site of Uf [Scarrow, R. C., Pyrz, J. W., & Que, L., Jr. (1990) *J. Am. Chem. Soc.* 112, 657-665] is corroborated, refined, and found to represent the diiron center of BSPAP as well.

Purple acid phosphatases (PAP's), a class of enzymes isolated from a wide variety of animal and plant sources, catalyze the hydrolysis of certain phosphate esters, including nucleotide di- and triphosphates and aryl phosphates in vitro (Antanaitis & Aisen, 1983; Doi et al., 1988; Vincent & Averill, 1990). The most thoroughly studied PAPs are the mammalian enzymes from porcine uterus (also called uteroferrin, Uf) (Antanaitis

et al., 1980, 1983) and bovine spleen (BSPAP) (Davis & Averill, 1982; Averill et al., 1987), which are glycoproteins with molecular mass of 35-40 kDa (Antanaitis & Aisen, 1983; Doi et al., 1988; Vincent & Averill, 1990). Uf consists of a single polypeptide chain, while BSPAP has two polypeptide chains which possibly arise from proteolysis during purification. The amino acid sequences of Uf and BSPAP exhibit greater than 90% homology (Hunt et al., 1987; Ketcham et al., 1989). The similarities in sequence and substrate specificity suggest that these enzymes may perform similar functions in vivo, despite the fact that Uf is an extracellular enzyme in porcine uterus while BSPAP is localized in bovine spleen cells.

[†]This work was supported by grants from the National Science Foundation (DMB-9104669 to L.Q.) and the National Institutes of Health (GM 32117 to B.A.A.). J.B.V. acknowledges the support of an NIH postdoctoral fellowship (GM 13500).